

# Towards Understanding and Harnessing the Effect of Image Transformation in Adversarial Detection

Hui Liu<sup>1</sup>, Bo Zhao<sup>1</sup>, Yuefeng Peng<sup>1</sup>, Weidong Li<sup>1</sup>, Peng Liu<sup>2</sup>

<sup>1</sup>School of Cyber Science and Engineering, Wuhan University, Wuhan

<sup>2</sup>College of Information Sciences and Technology, Pennsylvania State University, PA

{liuh824, zhaobo, yuefengpeng, chrisli}@whu.edu.cn, pliu@ist.psu.edu

## Abstract

Deep neural networks (DNNs) are threatened by adversarial examples. Adversarial detection, which distinguishes adversarial images from benign images, is fundamental for robust DNN-based services. Image transformation is one of the most effective approaches to detect adversarial examples. During the last few years, a variety of image transformations have been studied and discussed to design reliable adversarial detectors. In this paper, we systematically synthesize the recent progress on adversarial detection via image transformations with a novel classification method. Then, we conduct extensive experiments to test the detection performance of image transformations against state-of-the-art adversarial attacks. Furthermore, we reveal that each individual transformation is not capable of detecting adversarial examples in a robust way, and propose a DNN-based approach referred to as *AdvJudge*, which combines scores of 9 image transformations. Without knowing which individual scores are misleading or not misleading, *AdvJudge* can make the right judgment, and achieve a significant improvement in detection accuracy. We claim that *AdvJudge* is a more effective adversarial detector than those based on an individual image transformation.

## 1 Introduction

Adversarial attacks, which can generate images with small but maliciously-crafted perturbations to change the output of state-of-art classifiers, are still problematic for deep neural networks (DNNs). These perturbed images are referred to as adversarial examples [Szegedy *et al.*, 2014]. Adversarial attacks have proved to be a serious threat to DNN-based services in the physical world. For example, attackers who wear a pair of well-designed eyeglass frames can evade detection by facial recognition systems [Sharif *et al.*, 2016]. Attackers can project specifically crafted adversarial perturbations onto real-world objects, transforming them into adversarial examples [Lovisotto *et al.*, 2021].

The existence of adversarial examples raises great public concern and motivates research for an proactive defense.

These proactive defenses, e.g., adversarial training [Ding *et al.*, 2020], gradient masking [Lee *et al.*, 2021], etc., can harden DNN systems with small accuracy loss. However, it is shown in [Tan *et al.*, 2021] that hardened DNNs can still be evaded.

Due to the limitations of proactive defenses, reactive defenses, i.e., adversarial detection [Lust and Condurache, 2022] has attracted increasing interest of the research community. Unlike proactive defenses, adversarial detection only determines whether an input is benign or adversarial, without the need to identify the ground-truth label of an input.

Image transformation [Nesti *et al.*, 2021; Xu *et al.*, 2018; Liu *et al.*, 2021; Graese *et al.*, 2016; Bahat *et al.*, 2019; Tian *et al.*, 2018; Mekala *et al.*, 2019], which measures the disagreement of the DNN model in predicting the input and its transformed version, is one of the most effective approaches to detect adversarial examples. The main challenge of detecting adversarial examples via image transformation is to design appropriate transformation approaches, which should have the following two properties: (i) the DNN’s prediction on the adversarial example is significantly changed, and (ii) the DNN’s prediction on the benign example is unaffected. These two properties can be employed to identify the authenticity of the test image.

This paper systematically synthesizes (the knowledge gained through) the recent progress on adversarial detection via image transformations with a novel classification. Notably, we test the existing adversarial detectors based on image transformations against state-of-the-art adversarial attacks, and reveal a fundamental limitation of image transformation based detectors: no individual kind of image transformation has generic (i.e., can detect all kinds of adversarial attacks) detection ability. This key observation motivates us to answer a new research question: Is it possible to combine the strengths of each individual image transformation while avoiding their weaknesses? To answer this question, we propose to learn (the truth) from the individual detector scores without any prior knowledge about which individual scores are misleading. We design a DNN-based *AdvJudge*, and conclude that adversarial examples could be detected in a robust way by combining multiple transformations.

In summary, this paper makes the following contributions:

- To the best of our knowledge, we are the first to systematically review and test adversarial detection via image

transformations with a novel classification.

- We reveal that an individual image transformation has no generic ability to detect adversarial examples. Thus, we combine scores of 9 image transformations and design a DNN-based detector referred to as *AdvJudge*. Experimental results show that *AdvJudge* significantly outperforms all individual transformation detectors.

The remainder of this paper is organized as follows. Section 2 presents preliminaries on the adversarial attack and the prediction distance. In Section 3, we present a novel classification of image transformations for adversarial detection in the baseline architecture. Section 4 evaluates the performance of each of the image transformations in adversarial detection. In Section 5, we design and test the proposed detector *AdvJudge* that combines 9 image transformations. Finally, we conclude the paper in Section 6.

## 2 Preliminaries

### 2.1 Adversarial Attack

An adversarial attack [Carlini and Wagner, 2017; Goodfellow *et al.*, 2015; Kurakin *et al.*, 2017] is a unique form of attack in deep learning. Attackers mislead state-of-the-art DNN-based classifiers into making erroneous predictions by adding small perturbations to inputs. Most studies follow the formulation proposed by Szegedy *et al.* in [Szegedy *et al.*, 2014], where the generation of adversarial attacks is formulated as a minimization problem with the perturbation magnitude as the main constraint. That is,

$$\begin{aligned} \min \quad & \|\delta\|_p \\ \text{s.t.} \quad & f(x) \neq f(x') \\ & x' = x + \delta \in D \end{aligned} \quad (1)$$

where  $p$  norms include  $L_0$ ,  $L_2$  and  $L_\infty$  to measure the magnitude of the perturbation,  $\delta$  denotes the perturbation matrix that is added to the benign example  $x$  for synthesizing the adversarial example  $x'$ , which remains in the benign domain  $D$ . Function  $f(x) = y$  is a well-trained DNN model, which accepts an  $x \in \mathbb{R}^n$  and produces an output  $y \in \mathbb{R}^m$ .

Convolutional neural networks (CNNs) are the most widely used neural network architectures and have achieved incredible success in computer vision tasks. They are usually constructed by multiple convolutional layers and nonlinear activation functions, e.g., sigmoid, ReLU, and tanh.

### 2.2 Prediction Distance

The DNN prediction is usually a probability distribution. Existing approaches usually utilize Kullback-Leibler divergence ( $D_{KL}$ ) [Bahat *et al.*, 2019] to measure the distance between two probability distribution values. The definition of  $D_{KL}$  is formalized as Equation 2.

$$D_{kl}(Z(x)||Z(x_t)) = \sum Z(x) \log \frac{Z(x)}{Z(x_t)} \quad (2)$$

where  $D_{kl}$  is a measure of how a prediction distribution  $Z(x)$  of test image  $x$  is different from  $Z(x_t)$  of its transformed version  $x_t$ .

## 3 Image Transformation for Adversarial Detection

### 3.1 Baseline Detection Architecture

Adversarial examples yield significantly different outputs of the classifier under certain image transformations. In contrast, benign examples tend to yield robust and consistent classifications under these transformations. Given a test image  $x$  whose authenticity is unknown, an image transformation is performed to get its transformed version  $x_t$ . The test image  $x$  and its transformed version  $x_t$  are input to the DNN model. Then, this model produces two predictions,  $Z(x)$  and  $Z(x_t)$ . If the two predictions are far apart from each other, the test image is considered to be adversarial; otherwise, it is considered benign. Figure 1 shows the baseline architecture to detect adversarial examples via image transformations.

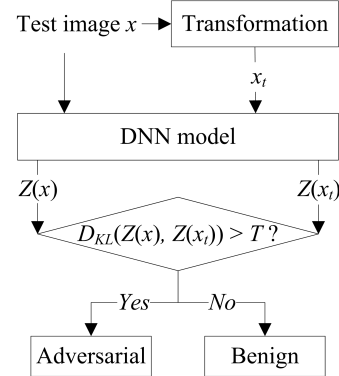


Figure 1: Baseline architecture to detect adversarial examples via image transformations.

Adversarial detection via image transformations has the following advantages: (i) they do not modify the architectures or parameters of the neural network and do not result in accuracy loss, (ii) they are independent of neural networks, and complementary to other defenses and detections, and (iii) they are simple, inexpensive, and so can be performed at runtime.

### 3.2 Taxonomy

In this subsection, we review the recent advances in adversarial detection via image transformations, and categorize them into two dimensions: pixel modification, and topological transformation.

#### Pixel Modification

Pixel modification is a kind of transformation that modifies the local or whole pixel values in an image. It can be divided into four groups: additive noise, smoothing, bit-depth reduction, and frequency-domain transformation.

(1) Additive noise: Image noise is a random variation of pixel values in an image. The most frequently occurring noises include Gaussian noise, Poisson noise, salt&pepper noise, etc. Gaussian noise is a statistical additive noise, which has a probability density function equal to that of the Gaussian distribution. In [Nesti *et al.*, 2021], Nesti *et al.* claimed

that adversarial examples that are robust to additive Gaussian noise may exist.

(2) Smoothing: Smoothing is a group of techniques widely used in image processing for reducing image noise. By selecting different mechanisms in weighting the neighboring pixels, the image smoothing method can be divided into the maximum, median, uniform, and Gaussian filters, etc [Xu *et al.*, 2018]. The maximum filter runs a sliding window over each pixel of the image, where the center pixel is replaced by the maximum value of the neighboring pixels within the window.

(3) Bit-depth reduction: Bit-depth reduction aims to reduce the information capacity of the image representation [Xu *et al.*, 2018]. Given an input  $x \in [0, 1]$ , to reduce  $x$  to  $i$ -bit depth ( $1 \leq i \leq 7$ ), the input  $x$  is multiplied by  $2^i - 1$  and then the result is rounded to an integer. Next the integer is scaled back to  $[0, 1]$  by dividing  $2^i - 1$ . The bit depth is reduced from 8 bits to  $i$ -bit with the integer-rounding operation.

(4) Frequency-domain: Many adversarial attacks attempt to modify pixels in ways that are usually imperceptible. High frequency patterns play a key role in the generation of adversarial examples [Zhou *et al.*, 2021]. Detection strategies based on the frequency-domain usually discard the high-frequency information of the image to “compress away” such adversarial perturbations. In particular, JPEG compression and its variants in [Kantaros *et al.*, 2020; Liu *et al.*, 2021] are shown to be an effective countermeasure to imperceptible adversarial examples.

## Topological Transformation

Topological transformation includes an affine transformation that preserves both the collinearity relation between points and ratios of distances along the line, and aims to change the pixel coordinates in an image to obtain a transformed version. The basic topological transformations include translation, flip, rotation, shear and scale.

(1) Translation: Translation is a simple topological transformation, which can be formulated as  $v' = v + \sigma$ , where  $v = [\mu, \nu]^T$  and  $v' = [\mu', \nu']^T$  represent the coordinates of a pixel in the original and transformed images, and  $\sigma = [\alpha, \beta]^T$  are horizontal and vertical translation parameters [Graese *et al.*, 2016].

(2) Flip: Image flip can be formulated as  $v' = Tv$ , where  $T \in \mathbb{R}^{2 \times 2}$  is a warping matrix, e.g.,  $T = \begin{bmatrix} -1 & 0 \\ 0 & 1 \end{bmatrix}$  in the horizontal flip. The effectiveness of the horizontal flip has been proved against C&W attacks under the known detector scenario [Bahat *et al.*, 2019].

(3) Rotation: Rotation has a formalized representation, e.g.,  $v' = Tv$  similar to flip, where  $T = \begin{bmatrix} \cos\theta & -\sin\theta \\ \sin\theta & \cos\theta \end{bmatrix}$ ,  $\theta$  is the rotation angle. The authors claimed in [Tian *et al.*, 2018] that their rotation-based detector achieved an accuracy of nearly 99% against C&W attacks in the white-box setting.

(4) Shear: Image shear refers to the linear transformation of each pixel to a fixed direction proportional to that of parallel lines in the plane. The horizontal shear can be formulated as  $v' = Tv$ , where  $T = \begin{bmatrix} 1 & a \\ 0 & 1 \end{bmatrix}$ , and  $a$  is a shear parameter.

Experiments in [Mekala *et al.*, 2019] demonstrated that horizontal shear was effective for adversarial detection.

(5) Scale: Scale can be expressed by the  $T = \begin{bmatrix} s & 0 \\ 0 & s \end{bmatrix}$ . The

scale parameter  $s > 1$  indicates the zoom-in transformation while  $s < 1$  indicates zoom-out. The zoom-in transformation yields an excellent ability to detect untargeted C&W attacks.

## 4 Performance of Image Transformations

### 4.1 Experimental Setup

We randomly choose 1,800 images from the ImageNet dataset [Russakovsky *et al.*, 2015] as benign images, and respectively yield 600 adversarial examples against the Inception V3 model by C&W [Carlini and Wagner, 2017], FGSM [Goodfellow *et al.*, 2015], and BIM attacks [Kurakin *et al.*, 2017]. Benign examples are divided into 1,440 training examples and 360 test examples. Each type of adversarial example includes 480 training examples and 120 test examples. For C&W attacks, the target class is the next class. The perturbation level  $\epsilon$  is set to 0.1 for both FGSM and BIM attacks. Note that the low perturbation level strictly limits the magnitude of adversarial perturbations, making adversarial detection more difficult. Pixel modifications and topological transformations are executed separately on benign examples and adversarial examples. Experimental results show the contribution of each image transformation to adversarial detection.

### 4.2 Threshold Setting

As shown in Figure 1, the appropriate threshold  $T$  is very important for the detection accuracy based on the baseline architecture. For this test, training examples are utilized to determine the appropriate threshold, and test examples are utilized to test the detection accuracy under this threshold.

It is time-consuming to determine an appropriate threshold  $T$  by a global search. To reduce the complexity, we calculate the  $D_{KL}$  value between training images and their transformed versions as the candidate set of the threshold. By iterating through the candidate set, we identify a threshold that maximizes the product of the TPR (true positive rate) and TNR (true negative rate) in training images. Under this threshold, we test the detection ability of the detector based on each individual image transformation against benign examples and three types of adversarial examples.

### 4.3 Pixel Modification Tests

We respectively select 50 random images from benign examples and each type of adversarial examples, and generate their transformed versions via pixel modification. Then, we compute the  $D_{KL}$  values between selected examples and their transformed versions. As shown in Figure 2, the  $D_{KL}$  values of benign and adversarial examples are plotted in color lines.

In Figure 2, the additive noise is realized by Gaussian noise with  $variance = 0$ , the maximum smoothing is a maximum filter with the  $3 \times 3$  sliding window, the bit-depth of images is reduced from 8 bits to 4 bits, and Feature-filter, one of the variants of the frequency-domain transform, is reproduced by

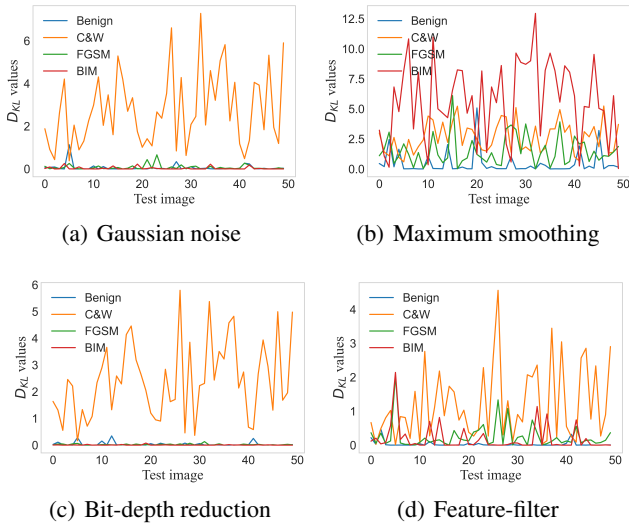


Figure 2: Distributions of  $D_{KL}$  values via pixel modification.

only reserving the  $0.7 \times 0.7$  low-frequency coefficients as described in [Liu *et al.*, 2021]. As shown in Figure 2, the  $D_{KL}$  values between benign images and their transformed versions are usually located at a lower level. These approaches via pixel modification are very effective for C&W attacks but are not always satisfactory against the other two attacks.

We test the performance of four groups of pixel modifications against three typical adversarial attacks. Table 1 lists the average  $D_{KL}$  values between test images (benign images and adversarial images generated by C&W, FGSM, and BIM attacks) and their transformed images. The average  $D_{KL}$  values of adversarial examples are usually greater than those of benign images. The results infer that adversarial examples (especially those generated by C&W attacks) are usually sensitive to pixel modifications, while benign images are immune to these operations. The detection accuracy under a certain threshold is also illustrated in Table 1. In general, the detectors based on pixel modification have an excellent ability to detect C&W attacks, but are relatively poor in detecting the other two attacks with low perturbation levels.

#### 4.4 Topological Transformation Tests

As shown in Figure 3, we also select 50 random images, and compute the  $D_{KL}$  values between test images (benign and adversarial images) and their transformed versions via topological transformation. The  $D_{KL}$  values of benign images are plotted in blue lines, and those of adversarial images are plotted in other colors.

In Figure 3, the translation parameters are set to  $[\alpha, \beta]^T = [5, 5]^T$ , the warping matrix  $T = \begin{bmatrix} -1 & 0 \\ 0 & 1 \end{bmatrix}$  indicates the horizontal flipping of the test image, the rotation angle  $\theta$  is set to  $20^\circ$ , and the shear parameter  $a = 0.3$ . The scale parameter  $s = 0.8$  indicates that the test images are shrunk by 0.8 times and then enlarged by 1.25 times to retain the same scale. This set of figures shows  $D_{KL}$  distributions of benign images are visibly lower than those of adversarial examples. The results

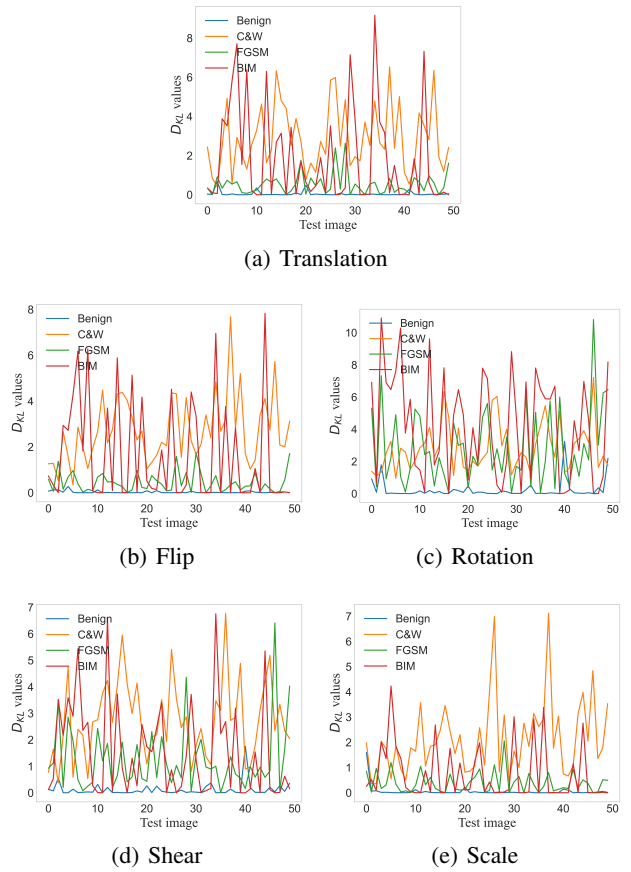


Figure 3: Distributions of  $D_{KL}$  values via topological transformation.

indicate that topological transformations could help to detect adversarial examples.

Similarly, we test the effect of topological transformations on adversarial detection with a given set of parameters. Table 2 lists the average  $D_{KL}$  values of the test images and the detection accuracy under a certain threshold. The average  $D_{KL}$  values of adversarial examples are always greater than those of benign examples. However, adversarial detection based on an individual topological transformation is still difficult. In particular, most adversarial examples based on BIM attacks can evade these detectors.

## 5 Joint Detection

Adversarial detector based on an individual image transformation cannot achieve satisfactory accuracy. How to improve the detection accuracy by combining the scores of multiple image transformations? To answer this question, we design a DNN-based detector referred as to *AdvJudge*.

### 5.1 Our Approach

*AdvJudge* is constructed by a simple DNN model. The implementation of this detector includes 3 steps: data preprocessing, constructing and training a DNN, and testing.

Transformation	Parameter	Threshold	Average $D_{KL}$				Accuracy			
			C&W	FGSM	BIM	Benign	C&W	FGSM	BIM	Benign
Additive noise	Gaussian	0.273	3.123	0.392	1.416	0.391	98%	45%	44%	<b>71%</b>
	Poisson	0.010	0	0.049	0.008	0.121	0%	<b>71%</b>	5%	42%
	Salt&Pepper	0.519	2.938	0.659	2.381	0.777	97%	42%	<b>54%</b>	67%
	Speckle	0.071	2.641	0.127	0.093	0.184	<b>100%</b>	48%	9%	68%
Smoothing	Gaussian	0.346	2.928	0.985	2.403	0.266	<b>100%</b>	68%	56%	82%
	Maximum	0.710	2.846	1.811	5.450	0.460	96%	71%	88%	79%
	Median	0.319	2.961	1.133	2.012	0.159	99%	<b>77%</b>	53%	<b>88%</b>
	Uniform	0.375	2.906	1.019	2.311	0.248	99%	70%	53%	83%
	Minimum	0.940	2.849	1.914	5.643	0.533	91%	70%	<b>90%</b>	83%
Bit-depth	4-bit	0.020	2.602	0.032	0.014	0.062	<b>100%</b>	41%	<b>9%</b>	67%
	5-bit	0.004	1.179	0.006	0.011	0.012	99%	42%	8%	68%
	6-bit	0.001	0.358	0.002	0.001	0.002	98%	<b>48%</b>	6%	<b>71%</b>
Feature-filter	0.6	0.170	2.340	0.614	0.252	0.097	98%	69%	<b>23%</b>	84%
	0.7	0.050	1.674	0.321	0.081	0.030	<b>99%</b>	82%	13%	84%
	0.8	0.011	0.788	0.118	0.022	0.005	<b>99%</b>	<b>87%</b>	13%	87%
	0.9	0.003	0.221	0.025	0.006	0.001	98%	84%	13%	<b>92%</b>

Table 1: Average  $D_{KL}$  values and detection accuracy via pixel modification.

(1) Data preprocessing. We combine 9 image transformations to obtain transformed versions, and calculates  $D_{KL}$  values between training images and their transformed versions. The framework of data preprocessing is plotted in Figure 4. For each training image, a feature vector  $V_{KL}$  consists of 9  $D_{KL}$  values. If the feature vector comes from an adversarial image, it is labeled 1; otherwise, it is labeled 0.

(2) Constructing and training a DNN. *AdvJudge* is a simple neural network that consists of fully connected layers. Details of this neural network are listed in Tab 3. This neural network is trained by the above feature vectors with labels.

(3) Testing. The test image is preprocessed as shown in Figure 4 to generate its feature vector. *AdvJudge* accepts the feature vector and gives a positive predictive value  $\rho$ . If  $\rho > 0.5$ , the test image is considered adversarial; otherwise, it is considered benign.

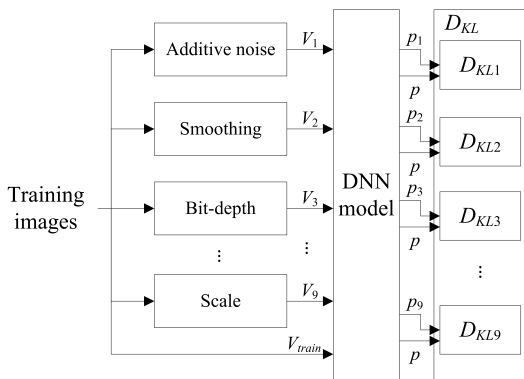


Figure 4: Data preprocessing.

ual transformations. As listed in Table 4, *AdvJudge* reports 92% precision and 94% recall. The F1 score is the harmonic mean of precision and recall, which is widely used to measure the success of a binary classifier. Compared to the best result among individual transformations, the F1 score of our detector achieves a 0.09 improvement.

Figure 5 shows ROC curves for detectors based on each image transformation and the joint transformation. It is shown that *AdvJudge*'s performance is better than those based on individual transformations. Additionally, the AUC measures are shown in Figure 5 for these 10 detectors. *AdvJudge* reports an AUC value of up to 0.97, which is significantly higher than the results among individual transformations. Therefore, we suggest that *AdvJudge* is able to effectively detect adversarial examples from a wide range of attacks.

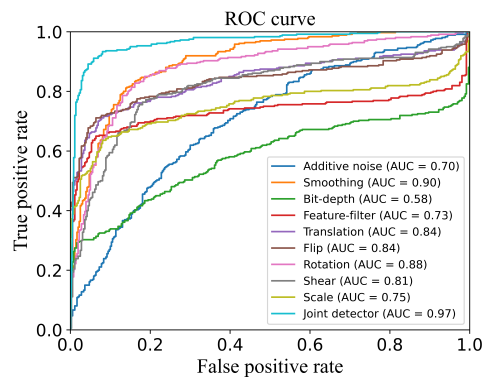


Figure 5: ROC curve.

## 5.2 Results

We utilize the same experimental setup in subsection 4.1 to train *AdvJudge*, and compare its performance with individ-

Transformation	Parameter	Threshold	Average $D_{KL}$				Accuracy				
			C&W	FGSM	BIM	Benign	C&W	FGSM	BIM	Benign	
Translation	1	0.083	2.618	0.461	0.455	0.030	<b>100%</b>	<b>78%</b>	32%	91%	
	3	0.228	2.982	0.607	0.981	0.056	99%	67%	<b>44%</b>	<b>93%</b>	
	5	0.227	3.039	0.678	1.202	0.067	98%	69%	<b>44%</b>	92%	
	7	0.193	3.004	0.685	0.994	0.069	<b>100%</b>	70%	42%	89%	
	9	0.224	3.034	0.713	1.062	0.078	98%	67%	41%	88%	
Flip	Vertical	1.095	2.646	2.402	2.622	1.352	93%	77%	65%	57%	
	Horizontal	0.130	3.003	0.601	0.820	0.056	<b>99%</b>	<b>80%</b>	41%	<b>88%</b>	
	Both	0.979	2.608	2.415	2.444	1.343	93%	79%	<b>66%</b>	58%	
Rotation	-30°	1.021	2.886	3.107	4.159	0.781	90%	83%	78%	75%	
	-20°	0.861	2.952	2.658	3.331	0.448	94%	<b>78%</b>	72%	85%	
	-10°	0.586	3.029	2.090	1.823	0.205	<b>96%</b>	74%	58%	<b>90%</b>	
	10°	0.420	3.043	2.070	1.803	0.204	<b>96%</b>	<b>78%</b>	52%	87%	
	20°	1.049	2.978	2.684	3.339	0.445	88%	<b>74%</b>	65%	87%	
	30°	1.003	2.951	3.178	4.269	0.740	93%	83%	79%	73%	
Shear	0.1	0.165	2.639	0.672	0.339	0.085	<b>98%</b>	76%	26%	<b>85%</b>	
	0.2	0.311	2.719	0.969	0.644	0.161	<b>98%</b>	73%	39%	<b>85%</b>	
	0.3	0.478	2.784	1.381	1.302	0.303	98%	78%	52%	83%	
	0.4	0.660	2.785	1.865	2.225	0.502	96%	<b>80%</b>	63%	80%	
	0.5	0.884	2.760	2.401	3.253	0.793	93%	<b>80%</b>	<b>71%</b>	72%	
Scale	0.8	0.127	2.404	0.531	0.260	0.063	<b>100%</b>	73%	<b>22%</b>	<b>89%</b>	
	0.9	0.109	2.144	0.391	0.142	0.048	<b>100%</b>	70%	17%	88%	
	1.1	0.070	1.754	0.290	0.082	0.032	<b>100%</b>	73%	13%	87%	
	1.2	0.050	1.622	0.277	0.070	0.027	<b>100%</b>	<b>75%</b>	8%	<b>89%</b>	

Table 2: Average  $D_{KL}$  values and detection accuracy via topological transformation.

Layer	Type	Activation	Output shape
Input			9
1	FC	Relu	64
2	FC	Relu	64
3	FC	Relu	64
4	FC	Relu	64
5	FC	Sigmoid	1

Table 3: Our detector architecture.

## 6 Conclusion

Image transformations help to detect adversarial examples. Such approaches are simple and inexpensive, and do not modify the architectures or parameters of the neural network. Therefore, a detector based on image transformations can be employed to detect adversarial examples at runtime without accuracy loss of the neural network. In this paper, we explore and test the effect of image transformation on adversarial examples generated by state-of-the-art adversarial attacks. The results demonstrate that an individual transformation has difficulty detecting adversarial examples in a robust way. This motivates us to develop a joint approach to improve detectability. We combine 9 image transformations to obtain their scores, and construct a set of feature vectors. A simple DNN learns these feature vectors to become a good judge. Experimental results show that our *AdvJudge* achieves a 0.92 F1 score and an AUC value of up to 0.97, which significantly outperforms all detectors based on an individual transforma-

Transformation	Parameter	Precision	Recall	F1 score
Additive noise	Gaussian	64%	66%	0.65
Smoothing	Maximum	85%	83%	0.83
Bit-depth	6	50%	64%	0.56
Feature-filter	0.9	65%	89%	0.75
Translation	1	70%	91%	0.79
Flip	Horizontal	73%	86%	0.79
Rotation	-10°	81%	84%	0.83
Shear	0.3	76%	81%	0.78
Scale	1.1	65%	85%	0.74
<i>AdvJudge</i>	All	<b>92%</b>	<b>94%</b>	<b>0.92</b>

Table 4: Performance of detectors.

tion.

## References

- [Bahat *et al.*, 2019] Yuval Bahat, Michal Irani, and Gregory Shakhnarovich. Natural and adversarial error detection using invariance to image transformations. *CoRR*, abs/1902.00236, 2019.
- [Carlini and Wagner, 2017] Nicholas Carlini and David A. Wagner. Towards evaluating the robustness of neural networks. In *2017 IEEE Symposium on Security and Privacy, SP 2017, San Jose, CA, USA, May 22-26, 2017*, pages 39–57, 2017.

- [Ding *et al.*, 2020] Gavin Weiguang Ding, Yash Sharma, Kry Yik Chau Lui, and Ruitong Huang. Mma training: Direct input space margin maximization through adversarial training. In *International Conference on Learning Representations*, 2020.
- [Goodfellow *et al.*, 2015] Ian J. Goodfellow, Jonathon Shlens, and Christian Szegedy. Explaining and harnessing adversarial examples. In *3rd International Conference on Learning Representations, ICLR 2015, San Diego, CA, USA, May 7-9, 2015, Conference Track Proceedings*, 2015.
- [Graese *et al.*, 2016] Abigail Graese, Andras Rozsa, and Terrance E. Boult. Assessing threat of adversarial examples on deep neural networks. In *15th IEEE International Conference on Machine Learning and Applications, ICMLA 2016, Anaheim, CA, USA, December 18-20, 2016*, pages 69–74, 2016.
- [Kantaros *et al.*, 2020] Yiannis Kantaros, Taylor J. Carpenter, Sangdon Park, Radoslav Ivanov, Sooyong Jang, Insup Lee, and James Weimer. Visionguard: Runtime detection of adversarial inputs to perception systems. *CoRR*, abs/2002.09792, 2020.
- [Kurakin *et al.*, 2017] Alexey Kurakin, Ian J. Goodfellow, and Samy Bengio. Adversarial examples in the physical world. In *5th International Conference on Learning Representations, ICLR 2017, Toulon, France, April 24-26, 2017, Workshop Track Proceedings*, 2017.
- [Lee *et al.*, 2021] Hyungyu Lee, Ho Bae, and Sungroh Yoon. Gradient masking of label smoothing in adversarial robustness. *IEEE Access*, 9:6453–6464, 2021.
- [Liu *et al.*, 2021] Hui Liu, Bo Zhao, Yuefeng Peng, Jiabao Guo, and Peng Liu. Feature-filter: Detecting adversarial examples through filtering off recessive features. *CoRR*, abs/2107.09502, 2021.
- [Lovisotto *et al.*, 2021] Giulio Lovisotto, Henry Turner, Ivo Sluganovic, Martin Strohmeier, and Ivan Martinovic. SLAP: Improving physical adversarial examples with Short-Lived adversarial perturbations. In *30th USENIX Security Symposium (USENIX Security 21)*, pages 1865–1882, 2021.
- [Lust and Condurache, 2022] Julia Lust and Alexandru Paul Condurache. Efficient detection of adversarial, out-of-distribution and other misclassified samples. *Neurocomputing*, 470:335–343, 2022.
- [Mekala *et al.*, 2019] Rohan Reddy Mekala, Gudjon Einar Magnusson, Adam Porter, Mikael Lindvall, and Madeline Diep. Metamorphic detection of adversarial examples in deep learning models with affine transformations. In *Proceedings of the 4th International Workshop on Metamorphic Testing, MET@ICSE 2019, Montreal, QC, Canada, May 26, 2019*, pages 55–62, 2019.
- [Nesti *et al.*, 2021] Federico Nesti, Alessandro Biondi, and Giorgio C. Buttazzo. Detecting adversarial examples by input transformations, defense perturbations, and voting. *CoRR*, abs/2101.11466, 2021.
- [Russakovsky *et al.*, 2015] Olga Russakovsky, Jia Deng, Hao Su, Jonathan Krause, Sanjeev Satheesh, Sean Ma, Zhiheng Huang, Andrej Karpathy, Aditya Khosla, Michael S. Bernstein, Alexander C. Berg, and Li Fei-Fei. Imagenet large scale visual recognition challenge. *Int. J. Comput. Vis.*, 115(3):211–252, 2015.
- [Sharif *et al.*, 2016] Mahmood Sharif, Sruti Bhagavatula, Lujo Bauer, and Michael K. Reiter. Accessorize to a crime: Real and stealthy attacks on state-of-the-art face recognition. In *Proceedings of the 2016 ACM SIGSAC Conference on Computer and Communications Security, Vienna, Austria, October 24-28, 2016*, pages 1528–1540, 2016.
- [Szegedy *et al.*, 2014] Christian Szegedy, Wojciech Zaremba, Ilya Sutskever, Joan Bruna, Dumitru Erhan, Ian J. Goodfellow, and Rob Fergus. Intriguing properties of neural networks. In *2nd International Conference on Learning Representations, ICLR 2014, Banff, AB, Canada, April 14-16, 2014, Conference Track Proceedings*, 2014.
- [Tan *et al.*, 2021] Jia Tan, Nan Ji, Haidong Xie, and Xueshuang Xiang. Legitimate adversarial patches: Evading human eyes and detection models in the physical world. In *MM '21: ACM Multimedia Conference, Virtual Event, China, October 20 - 24, 2021*, pages 5307–5315, 2021.
- [Tian *et al.*, 2018] Shixin Tian, Guolei Yang, and Ying Cai. Detecting adversarial examples through image transformation. In *Proceedings of the Thirty-Second AAAI Conference on Artificial Intelligence, (AAAI-18), the 30th Innovative Applications of Artificial Intelligence (IAAI-18), and the 8th AAAI Symposium on Educational Advances in Artificial Intelligence (EAAI-18), New Orleans, Louisiana, USA, February 2-7, 2018*, pages 4139–4146, 2018.
- [Xu *et al.*, 2018] Weilin Xu, David Evans, and Yanjun Qi. Feature squeezing: Detecting adversarial examples in deep neural networks. In *25th Annual Network and Distributed System Security Symposium, NDSS 2018, San Diego, California, USA, February 18-21, 2018*, 2018.
- [Zhou *et al.*, 2021] Yue Zhou, Xiaofang Hu, Jiaqi Han, Lidan Wang, and Shukai Duan. High frequency patterns play a key role in the generation of adversarial examples. *Neurocomputing*, 459:131–141, 2021.